A MULTI-OBJECTIVE APPROACH FOR MULTI-CHANNEL SAR DESPECKLING

Sergio Vitale[1]*, Hossein Aghababaei*[2]*,Giampaolo Ferraioli*[1]*, Vito Pascazio*[3]*, Gilda Schirinzi*[3]

[1]Università degli Studi di Napoli Parthenope, Dipartimento di Scienze e Tecnologie
[2] University of Twente, Faculty of Geo-Information Science and Earth Observation
[3]Università degli Studi di Napoli Parthenope, Dipartimento di Ingegneria

IGARSS 2021 - 2021 IEEE International Geoscience and Remote Sensing Symposium | 978-1-6654-0369-6/21/$31.00 ©2021 IEEE | DOI: 10.1109/IGARSS47720.2021.9553262

ABSTRACT

SAR image interpretation is always impaired by speckle that is a multiplicative noise due to interference among the backscatterings from targets inside a resolution cell. Many algorithms for both single and multi-channel SAR despeckling have been proposed in the last forty years following different approaches. Recently, a multi-objective convolutional neural network, named MONet, has been proposed for single channel SAR despeckling. It relies on a mulit-objectvie cost function that takes into account three main aspects of the SAR images: noise removal, details and statistics preservation. Inspired by MONet, in this paper a deep learning method for InSAR phase filtering is proposed. The idea is to benefit from the multi-objective cost function defined in MONet that seems to perfectly fit with the interferogram denoising. This is the first step towards a solution able to provide a complete processed multi-channel product.

Index Terms— SAR, Deep Learning, Denoising, Multi-Channel

1. INTRODUCTION

Multichannel SAR systems are composed of multiple antennas acquiring data from same scene with either a temporal or spatial shift. The data acquired by the single antenna are complex images whose amplitudes contain the backscattering information of the scene and phase embodies the range distance between the scene and the SAR.

Systems that exploit complex phase deriving from at least two complex SAR images are referred as interferometric SAR (InSAR) systems. While the amplitude is fundamental for the scene understanding while the difference between the (at least) two phases (interferogram) allows to retrieve different information such as scene's height profile, deformation of the earth's surface and topographical signals [1]

Therefore, InSAR products are very useful for a complete understanding of the scene. The problem lies in the difficult interpretation of the InSAR products: first, the amplitude images are characterized by the presence of a multiplicative noise called speckle impairing the interpretation [2]; second, interferograms are provided in their wrapped shape (in the interval $(-\pi, \pi)$) hiding the real value of the phases; third, the interferograms are affected by noise related to the coherence among the acquisitions (closer are the acquisitions higher is the coherence and less is the noise) [3]. A method for producing a complete clean InSAR product is crucial for further task such as scene classification, segmentation, detection, and height retrieval applications (tomography, DEM, etc...). The aim of this paper is to extend a recently proposed method for single SAR amplitude image despeckling (MONet [4]) to the multi-channel case (i.e. two or more SAR complex images). In particular, we propose to extend the network to the interferogram filtering, as first step towards a complete and unique solution for multi-channel SAR framework.

2. MONET

In this paper the backbone of the MONet architecture and its multi-objective cost function have been considered. In particular, the original version of MONet is a seventeen CNN for SAR amplitude image despeckling whose training relies on a synthetic dataset, where an optical image serves as noise-free reference X and the noisy input Y is obtained by multiplying X with a speckle realization simulated under the fully developed hypothesis. The architecture of MONet is shown in Figure 1: it is composed of seventeen convolutional layers, interleaved by a skip connection every two layers, followed by the Rectified Linear Unite (ReLU) [5] after (except the last) and with batch normalization [6] only in the inner layers.

The main aspect of MONet is the definition of a multi-objective cost function taking care different aspects of the filtering process. In particular, the cost function is composed of three terms: $\mathcal{L}_2$ computes the mean square error (MSE) between the filtered output $\widehat{X}$ and the reference X; $\mathcal{L}_\nabla$ computes the MSE between the gradient of $\widehat{X}$ and X; $\mathcal{L}_{KL}$, through the the Kullback-Leibler divergence, estimates the distance of the distribution of the estimated noise $\widehat{N} = Y/\widehat{X}$ and the Rayleigh distribution of the fully developed speckle. These three terms allow the network to balance the noise suppression and detail preservation: the $\mathcal{L}_2$ helps in removing noise, while $\mathcal{L}_\nabla$ and $\mathcal{L}_{KL}$ tend to preserve spatial details and statistical properties, respectively.

3. THE MODEL

In a multi-channel SAR framework the dataset is composed by at least two complex SAR images. In this paper we consider a two-channel system. Let us define $Z_1 = A_1 \exp(j\psi_1)$ and $Z_2 = A_2 \exp(j\psi_2)$ two complex SAR images, with A_1 and A_2 being the amplitudes and ψ_1 and ψ_2 being the phases, respectively. It is widely known that by multiplying the first image by the complex conjugate of the second one and by taking the phase of the result, it is possible to extract the so-called interferometric phase ϕ (i.e. the difference between the two phases). It follows that, in a two-channel framework, the useful parameters that can be estimated or restored are three: the two amplitudes A_1 and A_2 and the interferometric phase ϕ. As a first step towards a complete and unique solution for multi-channel SAR framework, in this paper we focus on the latter.

Let us consider the noise free (wrapped) interferometric phase ϕ, and let us define ϕ_n the noisy measured (wrapped) interferometric phase. The relation between the two interferometric phases can be characterized by an additive model [7]:

$$\phi_n = \phi + n \tag{1}$$

where n is a zero-mean noise. In Eq.(1), the original phase and the noise are assumed to be independent from each other.

Given the statistical distribution of the noise, the probability density function of the measured phase, given the actual noise free one is given by [3]:

$$P_{\Phi_n}(\phi_n) = \frac{1}{2\pi} \frac{1-\gamma^2}{1-\gamma^2\cos^2(\phi_n-\phi)} \cdot \cdot \left(1 + \frac{\gamma\cos(\phi_n-\phi)\cos^{-1}(-\gamma\cos(\phi_n-\phi))}{(1-\gamma^2\cos^2(\phi_n-\phi))^{1/2}}\right) \tag{2}$$

where γ is the absolute value of the coherence coefficient.

4. PROPOSED METHOD

MONet has shown that the filtering process works well mainly when the testing cases match the statistical distribution used in the training dataset [4]. Inspired by this outcome, the aim of this paper is to take advantage of the MONet scheme for the InSAR phase filtering.

Starting from several DEM SRTM, a wrapped phase ϕ has been simulated using different baselines B. The wrapped noisy phase ϕ_n has been obtained using the additive model of Eq. (1). The noise has been simulated using different coherence values γ. Considering the formalism of MONet, in this context, the noise-free phase serves as reference of the network $X = \phi$, while the noisy phase serves as input $Y = \phi_n$.

The MONet cost function of Fig. (1) needs to be particularised to the considered case. The $\mathcal{L}_{KL}(N, \hat{N})$ term is computed between the known statistical distribution of the noise N, derived from Eq. (2), and the statistical distribution of the difference image $\hat{N}$, obtained from Y and $\hat{X}$. Concerning the $\mathcal{L}_2(X, \hat{X})$ and the $\mathcal{L}_\nabla(X, \hat{X})$ terms , they are computed using the noise free interferometric phase X, and the estimated noise free phase $\hat{X}$. Summarizing, the proposed network is mainly the same as the classical MONet one, shown in Fig. (1) except for the different definition of the input and reference and considering a difference operation instead of a ratio one in the Loss Function (KL term).

4.1. Experiments

Seven different DEM SRTM have been used for constructing the dataset. From each of them, wrapped noisy phases with three values of coherence $\gamma = [0.5, 0.7, 0.9]$ and three different baselines $B = [40, 60, 90]$ meters have been simulated. In total, $120,000$ patches of dimension 128×128 have been extracted.

In order to test the proposed method a noisy interferogram with baseline $B = 60$ and three values of $\gamma = [0.5, 0.7, 0.9]$ have been simulated for adding the noise according to the above description.

In order to validate the method, a comparison with other state of art solution has been carried out: Box Car, Goldestein [8], NL-InSAR [9] and InSAR-BM3D [10]. The first four have been tested using the free on-line framework[11] and the default values here indicated have been used for the filters. For the last, the implementation of the authors and their default values have been considered. Moreover, constant amplitude images have been considered for those filters that require them in addition to the interferograms. Results are shown in Figure 2. From the filtered phase with $\gamma = 0.9$ appears that MONet, toghether with NL-InSAR, is the best in preserving the fringe's shape, while InSAR-BM3D tends to produce some artefacts in correspondence of the tiniest ones. Goldestein is still noisy, while BoxCar delete some details even if the average quality is high. With the decreasing of the coherence $\gamma = [0.7, 0.5]$, and the consequent augment of noise level, the drawbacks of Goldstein and Boxcar are more evident. NL-InSAR begins to suffer tiny fringes producing many artefacts and deleting important details. InSAR-BM3D is almost stable even if its behaviour on tiny fringes is slightly more accentuated. MONet is able to better preserve the shape of the fringes with respect to all the other methods but tends to produce more smoothed results limiting the dynamic of the output. To better spot the differences among the filters, the residual images where the absolute difference among the reference phase and filtered ones are shown in Figure 3. The zero difference is set on gray level.

It can be noted how MONet and NL-InSAR tends to produce stronger differences with the increasing of the coherence. Similarly, even if attenuated, happen for InSAR-BM3D. In particular, it is possible to note that in all cases NL-InSAR and InSAR-BM3D produce stronger errors (black and white

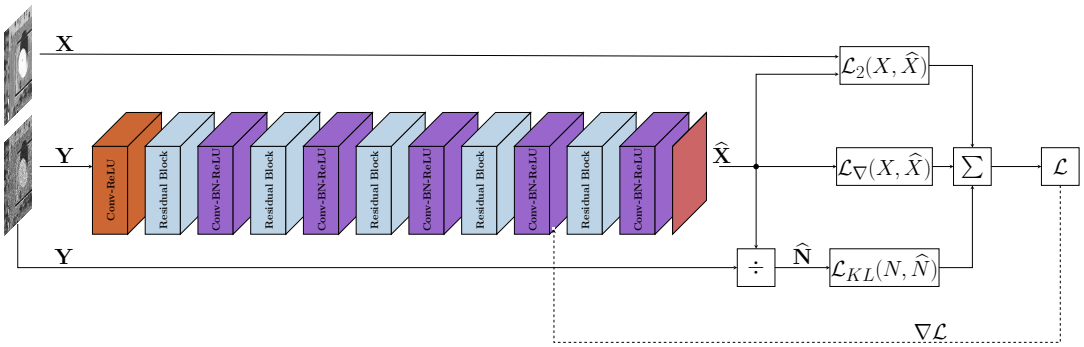

Fig. 1. Architecture of MONet: first convolution layer followed by a ReLU, after that a series of fifteen convolutional layers with ReLU and Batch are present alternated with a skip connection every three layers; at the end a simple convolutional layer. On the right the composition of the cost function is described.

structures) in correspondence on the edges of the fringes than MONet.

These outcomes are confirmed from the numerical evaluation shown in Table 1 where the averaged values of the MSE, the SSIM and the FOM have been computed on the three shown test cases. All the metrics confirm that InSAR-BM3D and MONet are the most competitive ones. In particular, MSE and FOM confirm the good preservation of the interferogram details and edges from MONet.

	MSE	SSIM	FOM
BoxCar	1.61	0.58	0.83
Goldenstein	2.99	0.31	0.83
InSAR-BM3D	<u>1.23</u>	**0.67**	<u>0.87</u>
NL-InSAR	1.89	0.52	0.84
MONet	**0.86**	<u>0.66</u>	**0.97**

Table 1. Numerical evaluation carried out on the three test cases.

5. CONCLUSION

In this paper a CNN based solution for InSAR phase filtering has been proposed. The aim is to move the first step towards a solution that can provide a complete processing of multi-channel SAR products. To this goal, the single SAR image despeckling algorithm MONet has been extended to the interferogram phase filtering. Inspired by the good results of MONet, the idea is to take advantage from its architecture and its multi-objective cost function. The results, compared with other State-of-Art methods, show a good performance mainly on the preservation of the fringe's shape while some difficult arise in the dynamic management. Future work will focus on the joint elaboration of SAR amplitude and phase

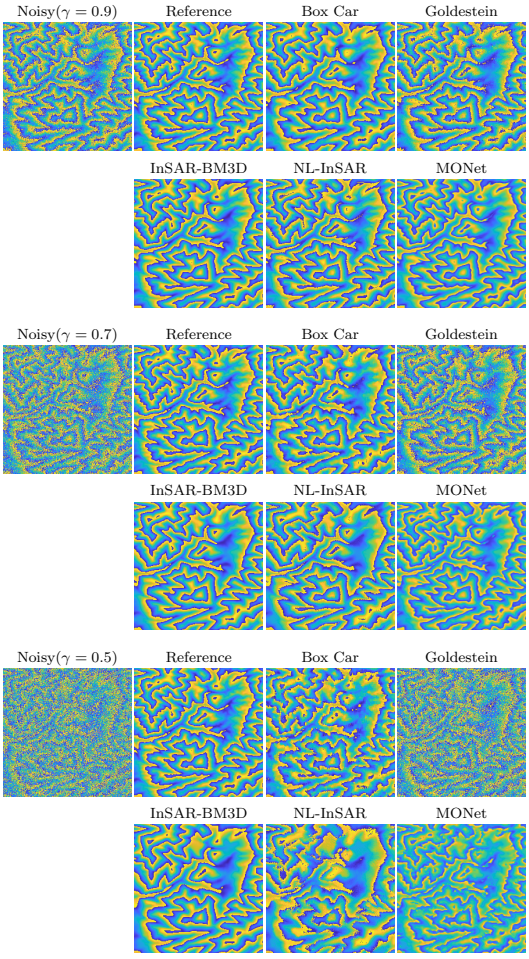

Fig. 2. Result on simulated interferograms. Three noisy interferograms have been testes with three different coherence values: $\gamma = 0.9$ in the top, $\gamma = 0.7$ in the middle, $\gamma = 0.5$ in the bottom.

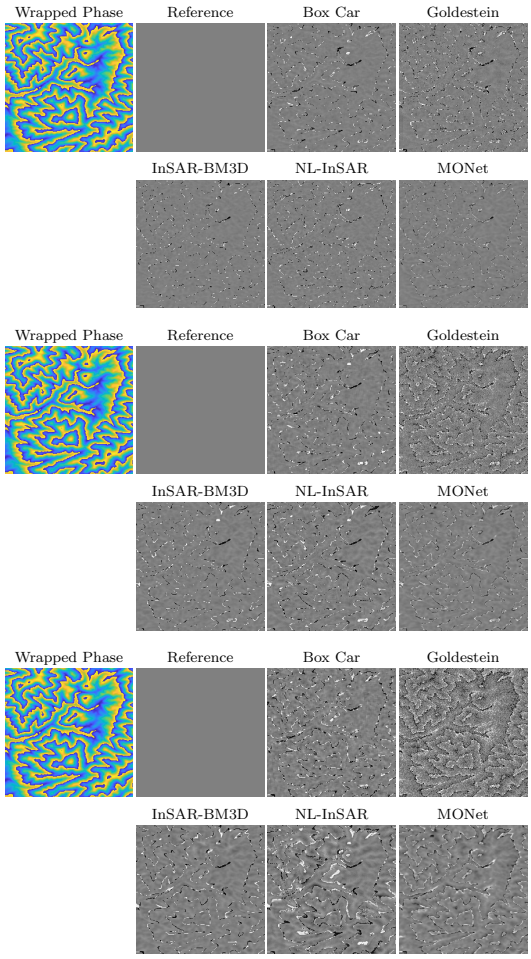

Fig. 3. Absolute difference among reference interferograms and filtered ones. Results on the three different coherence values are shown: $\gamma = 0.9$ in the top, $\gamma = 0.7$ in the middle, $\gamma = 0.5$ in the bottom.

data in order to produce a complete multi-channel processed product.

6. REFERENCES

[1] G. Fornaro and V. Pascazio, "SAR Interferometry and Tomography: Theory and Applications," *Academic Press Library in Signal Processing, Elsevier*, 2013.

[2] F. Argenti and L. Alparone, "Speckle removal from sar images in the undecimated wavelet domain," *IEEE Transactions on Geoscience and Remote Sensing*, vol. 40, no. 11, pp. 2363–2374, 2002.

[3] R. Bamler and P. Hartl, "Synthetic Aperture radar interferometry," *Inverse Problem*, vol. 14, pp. R1–R54, August 1998.

[4] S. Vitale, G. Ferraioli, and V. Pascazio, "Multi-objective cnn-based algorithm for sar despeckling," *IEEE Transactions on Geoscience and Remote Sensing*, pp. 1–14, 2020.

[5] Alex Krizhevsky, Ilya Sutskever, and Geoffrey E Hinton, "Imagenet classification with deep convolutional neural networks," in *Advances in Neural Information Processing Systems 25*, F. Pereira, C. J. C. Burges, L. Bottou, and K. Q. Weinberger, Eds., pp. 1097–1105. Curran Associates, Inc., 2012.

[6] Sergey Ioffe and Christian Szegedy, "Batch normalization: Accelerating deep network training by reducing internal covariate shift," *CoRR*, vol. abs/1502.03167, 2015.

[7] C. Lopez-Martinez and X. Fabregas, "Modeling and reduction of sar interferometric phase noise in the wavelet domain," *IEEE Transactions on Geoscience and Remote Sensing*, vol. 40, no. 12, pp. 2553–2566, 2002.

[8] Richard M. Goldstein and Charles L. Werner, "Radar interferogram filtering for geophysical applications," *Geophysical Research Letters*, vol. 25, no. 21, pp. 4035–4038, 1998.

[9] Charles-Alban Deledalle, Loïc Denis, and Florence Tupin, "Nl-insar: Nonlocal interferogram estimation," *IEEE Transactions on Geoscience and Remote Sensing*, vol. 49, no. 4, pp. 1441–1452, 2011.

[10] Francescopaolo Sica, Davide Cozzolino, Luisa Verdoliva, and Giovanni Poggi, "The offset-compensated nonlocal filtering of interferometric phase," *Remote Sensing*, vol. 10, no. 9, 2018.

[11] "Despeckcl," `https://github.com/gbaier/despeckCL`, Accessed: 2021-05-20.